13B.1 3 km WRF simulations of convective initiation with and without the Kain-Fritsch Scheme

Jeffrey D. Duda and William A. Gallus Jr.
Iowa State University

I. Introduction

With grid spacings of O(1 km) becoming increasingly common in operational and mesoscale modeling, the issue of whether or not to use a convective parameterization scheme (CPS) is becoming more important. This range of grid spacings is one for which a solution to the problem may not exist, since traditional CPSs were usually designed for use at grid spacings greater than 50 km, grid spacings of O(100 m) are required to fully resolve convective structure (Bryan et al. 2003), and the hybrid approach to convection parameterization was designed for use on grid spacings of 20 – 50 km (Molinari and Dudek 1992). The Kain-Fritsch (KF) CPS is based on the Fritsch-Chappell (Fritsch and Chappell 1980) scheme that was designed to be used at 10-30 km and assumes that the updraft and downdraft may comprise a significant area of a grid column. The KF scheme uses CAPE removal as a closure. It uses a convective trigger function based on a temperature perturbation of a 50-mb mixed layer parcel at its lifting condensation level (LCL) as well as the grid-resolved vertical velocity at the LCL to determine whether or not to activate the scheme in a grid column. This trigger function has been shown to be the most successful at 25 km grid spacing, but an assumption of linear dependence of model resolvable vertical motion on grid spacing can extend the use of the scheme to a wide range of grid spacing values.

A number of studies have shown the KF scheme to generally outperform other CPSs such as the Betts-Miller-Janjic and Grell-Devenyi schemes that are available with the Weather Research and Forecasting (WRF) model (Gilliland and Rowe 2007; Wang and Seaman 2007; Ma and Tan 2009). Gilliland and Rowe (2007), for example, showed that the KF scheme could more accurately depict the characteristics of an isolated supercell in 3-D idealized case as well as those of scattered summertime convection at 4 km. Not only did the KF scheme outperform other schemes, but it also outperformed the 4 km simulation that used no convective scheme, thus indicating that the KF scheme in particular can be used to improve forecasts even at such high resolutions. This generalization is also supported by the results of Lean et al. (2008) who showed a 4 km model simulation had difficulty accurately representing convection, particularly regarding initiation timing.

With evidence that the KF scheme can improve model simulations at high resolutions and the relative lack of computer resources needed to run a mesoscale model at sufficiently high resolution to unarguably resolve deep moist convection explicitly, this investigation aims to determine whether or not the KF scheme is also effective at 3 km grid spacings, as well as whether or not modifications to the KF code can be made to improve the forecast of warm-season mesoscale convective systems (MCS) over not using a CPS.

2. Methodology

The WRF-ARW model, version 3.1.1 was used to conduct a series of five simulations for each of 12 cases of warm-season MCSs across the U.S. The five simulations include: 1) one with no convective scheme used (denoted frequently in this study as “control”); 2) one with the KF scheme used as is (“KF orig” or “KF control”); 3) one with the trigger scheme altered to remove the linear dependence of vertical motion on grid spacing (“KF nodx”); 4) one in which the three main inputs to the KF scheme, vertical motion (W), temperature (T), and water vapor mixing ratio (Q) were averaged over 5 x 5 non-overlapping grid boxes prior to being passed into the KF subroutine (“KF 5x5 ave WTQ”); and 5) one in which the heat and moisture tendencies as well as the convective time step precipitation rate output from the KF scheme were averaged over 5 x 5 non-overlapping grid boxes (“KF 5x5 ave tend”). These last two simulation types were chosen to essentially fool the KF scheme into thinking it was actually running at 15 km grid spacing instead of at 3 km, to investigate if this might lead to an improved forecast. The simulations were run on a one-way nested pair of domains

Corresponding author address: Jeffrey D. Duda, 3134 Agronomy Hall, Iowa State Univ., Ames, IA; E-mail: jdduda@iastate.edu

with the 3 km grid nested inside a 12 km grid with a 3000 km x 3000 km size. The 3 km domain was variable in shape, but had an area equivalent to that of one approximately 1000 km x 1000 km in size. This was done to reduce the influence of the domain boundaries on the interior of the domain. The coarse and fine grid time steps were 36 and 9 s, respectively. The Mellor-Yamada-Janjic scheme was used for boundary layer parameterization. The Thompson scheme was used for microphysics. Simulations used NAM analysis data for initial and lateral boundary conditions, which were fed into the model every six hours. Each simulation was run for 24 hours. Most, but not all, of the simulations were initialized at 1200 UTC. Initialization time was selected such that initiation of the target MCS occurred within the 6 – 9 hour forecast period, a long enough time after initialization such that spin-up issues would be reduced or eliminated.

Verification of the model runs was performed using the Method for Object-based Diagnostic Evaluation (MODE) tool offered as part of the Model Evaluation Tools (MET) package from the WRF Developmental Testbed Center. As its name suggests, MODE creates objects from a data set using user-controlled settings. It then uses fuzzy logic to compute the likelihood (expressed as a parameter between 0 and 1 called "interest") that an object in the forecast field is the same as a corresponding object in the observation field. Precipitation was chosen as the field over which to verify. Stage IV multi-sensor precipitation data from NCEP/NCAR were used as the observations. Since the focus of the investigation was on initiation of convection, 1-hr and 6-hr accumulated precipitation intervals starting at convective initiation (CI) were used. In this study, CI was defined as the first occurrence of 1-hr precipitation greater than 3 mm. Since model output was 15 minutes, this allowed for higher temporal resolution than the Stage IV data, which were available at 1 hour intervals. Therefore, timing errors in initiation were limited to one hour bins. It should be noted that the threshold value used to define objects in MODE was held constant for each of the simulations within each case, but may have varied among the 12 cases. The most commonly used value was 1.27 mm.

Various skill scores were used to rate each simulation. Since it has been shown that some traditional skill scores such as the equitable threat score (ETS) can double penalize a forecast that has only a displacement error (among other ways it can excessively penalize an otherwise better forecast than what the score indicates, especially for high-resolution forecasts), some non-traditional skill measures that are output from MODE were used as well as ETS and bias for comparison. These other scores include the median of maximum interest (MMI), which is computed as the median of the set of maximum interest values compiled from a larger set of interest values between *all* pairs of objects between the forecast and observation fields, the interest value between *key* objects (i.e., the objects that represent CI), and some other object-based parameters. These other parameters include the average (across all objects in one data set) 50^{th} percentile rain intensity value, total precipitation volume, area of objects, and centroid distance between all matched objects (pairs of objects in the forecast and observation data sets are matched when the interest value between them exceeds a certain value, 0.7 in this study). The centroid displacement (i.e., location error) at initiation was also monitored.

3. Results

An example of output from the runs compared to observations can be found in Fig. 1. This section will be sorted by the 1-hr accumulation results first, then the 6-hr accumulation results.

3.1 1-hr accumulation

Table 1 shows the means and standard deviations of the differences between values for some of the skill measures for a given run and that of the control run. This enables a faster way of comparing the KF runs to the no KF run. Since many of the scores are being compared to that of the control run, it makes sense to see the multitude of 0.0 values in the top row of Tables 1a,b. Perhaps more interesting than the values in Table 1a are those in Table 1b which indicate that the spread in each score among the different cases is very large, on the order of the individual scores themselves (not shown). This is likely due, at least in part, to the small sample size: 12 cases are too few to be able to say anything about statistical significance. Nonetheless, when summing the ranks of the values in Table 1a, the following results are obtained (sum of ranks in parentheses):

1) KF 5x5 ave tend (16)
2) KF orig (21)
   KF nodx (21)
4) control (22)
5) KF 5x5 ave WTQ (25)

This list of ranks of sums indicates that the KF 5x5 ave tend run has more skill using 1-hr precipitation, while the KF 5x5 ave tend run has the least skill among the five run types. However, the KF orig run had the smallest location error at initiation with 115 km on average. The control run was a close second with an average of 124 km. The remaining three runs had average location errors of 148, 150, and 151 km for the KF 5x5 ave tend, KF nodx, and KF 5x5 ave WTQ runs, respectively.

Although timing errors have a much lower resolution, as described in section 2, it was still clear that all of the run types initiated convection early on average. While some of the runs did initiate convection late in some of the cases, when this happened it was only by one or two hours. When initiation occurred early, it was sometimes by as much as four to five hours. It is unknown as to why the runs initiated so early. However, when comparing the runs to each other instead of the observations, it is clear that the KF 5x5 ave WTQ and KF 5x5 ave tend runs initiated earlier than the control or KF orig runs. The KF nodx run was in the middle. It is likely that a change to the trigger function in the KF scheme code is partially responsible for this. The trigger function has the formula

$$\delta T = k * \left[w_g - c(z)\right]^{1/3},$$

where δT is a temperature perturbation of a potential updraft parcel with temperature T_{parcel} at its LCL, w_g represents the running mean grid resolved vertical velocity, and

$$w_g = w_{LCL} * {}^{DX}/_{25},$$

where DX is the grid spacing in kilometers. The

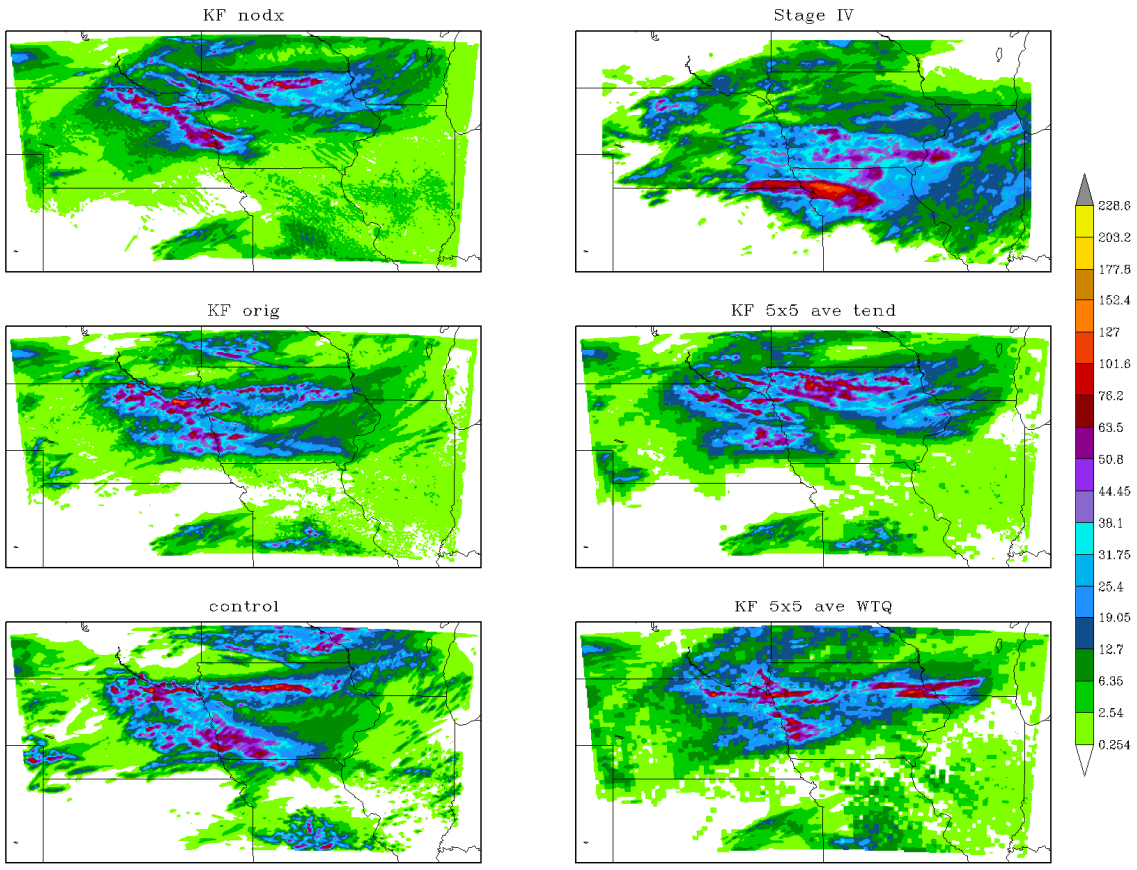

Figure 1. Accumulated precipitation from initiation to 1200 UTC 02 June 2010. In most of the runs for this case, this amounts to about 18 hours of accumulated precipitation. Contours are in units of mm.

Table 1a. Average difference between skill scores of various run types and those of the control run for 1-hr precipitation accumulation at initiation. The scores labeled with "error" represent the difference between the value of that score for each run type and that of the observations. Mean INTENSITY_50 represents the average of the 50th percentile of precipitation values of each object for the entire data set. Mean INTENSITY_SUM represents the average of the total volume of precipitation in each object for the entire data set. Mean CENTROID_DIST represents the average distance between centroids of matched object pairs between the forecast and observation data. The other skill measures have already been introduced or defined. Values highlighted in red are the worst score for the skill measure, while those in green are the best score. *-The values for the bias scores are the average bias score across all cases for each run and are not compared to the control run.

Run	MMI	Mean INTENSITY_50 error (mm)	Mean INTENSITY_SUM error (mm)	Mean area error (km^2)	Mean CENTROID_DIST (km)	Bias*	ETS
Control	0.0000	-0.374	-243.66	-533.48	0.00	1.69407	0.00000
KF orig	-0.0269	-0.413	-241.18	-262.72	2.51	2.24626	0.00592
KF nodx	-0.0389	-0.366	-134.19	1014.44	-13.14	4.37019	0.00362
KF 5x5 ave WTQ	-0.0606	-0.082	-311.63	70.99	-7.07	4.69288	-0.00073
KF 5x5 ave tend	-0.0292	-0.343	-167.77	340.19	-11.61	3.28763	0.00786

Table 1b. As in Table 1a except for standard deviation.

Run	MMI	Mean INTENSITY_50 error (mm)	Mean INTENSITY_SUM error (mm)	Mean area error (km^2)	Mean CENTROID_DIST (km)	Bias*	ETS
Control	0.0000	0.569	1339.15	2433.62	0.00	1.71530	0.00000
KF orig	0.0401	0.401	1351.40	2545.94	40.09	1.25772	0.02695
KF nodx	0.0689	0.381	1334.43	2918.38	32.83	2.66854	0.03455
KF 5x5 ave WTQ	0.0492	0.326	1221.56	2490.99	62.94	2.72908	0.03591
KF 5x5 ave tend	0.0664	0.385	1432.61	3003.63	43.63	2.42453	0.04700

scheme activates when $T_{parcel} + \delta T > T_{env}$ for environmental temperature T_{env} (Kain 2004). In the KF orig and KF 5x5 ave tend runs, DX = 3 km. But in the KF nodx and KF 5x5 ave WTQ runs, DX = 15 km. The DX/25 factor is there due to the assumption that resolvable vertical motion is linearly dependent on grid spacing. This assumption may not be true. A series of idealized squall line simulations were run using the two-dimensional version of the WRF with the initial sounding dried to the point where no deep moist convection occurred and no precipitation fell. The maximum vertical motion was then extracted from each run. The results are summarized in Fig. 2. All caveats due to the differences between 2D idealized and 3D real-data WRF simiulations aside, the relationship does not appear to be linear in the 3 – 15 km range. In fact, the relationship appears more exponential in nature. Regardless, even though all of the simulations used 3 km grid spacing outside of the KF scheme, the DX/25 factor in the trigger function is more friendly to DX = 15 km than to DX = 3 km. Thus, the KF scheme is more readily activated when DX = 15 km than when DX = 3 km. The initiation timing tendencies support this conclusion.

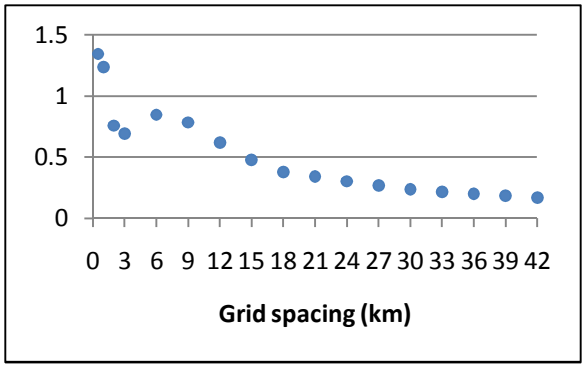

Figure 2. Maximum resolved vertical velocity (ms^{-1}) as a function of grid spacing for a series of 2D WRF simulations run dry so that no precipitation fell.

When comparing the interest values between key objects, the control run was the best, followed by the KF 5x5 ave tend, KF orig, KF 5x5 ave WTQ, and KF nodx runs. Although skill measures such as MMI and average CENTROID_DIST provide an objective evaluation of the forecast as a whole, since the focus of this investigation is on initiation of a target MCS, the location and timing errors at initiation, as well as the interest value between key objects provide a better indication of the forecast skill. What these additional skill measures do for overall evaluation of the different run types is make the control and KF orig runs look better than when the sum of ranks was computed. Thus, for 1-hr precipitation accumulation, the KF 5x5 ave tend, KF orig, and

control runs look to be the best and are difficult to distinguish by skill scores.

3.2 6-hr accumulation

Although the focus of the study is on initiation of MCSs, a well-simulated initiation does not necessarily lead to a well-simulated MCS. In an attempt to verify the early stages of convective development leading up to formation of an MCS, the same skill scores were also computed using a 6-hr accumulation period. Table 2 shows the means and standard deviations for the same skill measures as in Table 1. Table 2 shows very similar features as did Table 1, namely, very large spread in the scores relative to the values in each case (not shown). The sum of ranks for this set of scores is:

1) KF orig (13)
2) control (15)
3) KF nodx (25)
   KF 5x5 ave WTQ (25)
5) KF 5x5 ave tend (27)

This ranking is much different than that for 1-hr precipitation scores. It indicates that the runs with modified KF code did considerably worse than the KF orig and control runs.

When interest between key objects is evaluated, the control, KF orig, and KF 5x5 ave tend runs are 1, 2, 3, respectively, but the averages are close. For 6-hr precipitation overall, it seems the control and KF orig runs performed the best. These results agree with those of a subjective analysis performed for each of the simulations as well, which ranked the control and KF orig runs at the top two, separated by only one rank in the sum of ranks. The KF 5x5 ave tend run was third in the subjective evaluations.

4. Discussion

A more detailed analysis of the simulations was performed to determine if there was any systematic difference which may be responsible for the different initiation times, locations, and model skill. Some specific aspects of the analysis are now discussed.

Model soundings were taken from the centroid of 1-hr precipitation at the location of initiation from a period of 90 minutes leading up to initiation. These soundings revealed more similarities than differences between the different runs. For example, the soundings from all of the runs showed cooling and moistening of the layer between about 50 – 75 mb above ground to about 750 – 700 mb. The degree of balance between moistening and cooling was dependent on case. This is not remarkable, since most of the cases modeled convection that initiated in the late afternoon during the warm season. Thus, this cooling and moistening is probably showing the evolution of an unstable boundary layer and the lower free atmosphere, with strong diabatic heating at the surface. However, these soundings also revealed a tendency for the entire capping layer to fully erode before initiation in the control and KF orig runs, but not necessarily in the KF 5x5 ave WTQ and KF 5x5 ave tend runs, as in some cases there was still substantial CIN at initiation in those runs. This tendency could be explained

Table 2a. As in Table 1a except for 6-hr precipitation accumulation starting at initiation.

Run	MMI	Mean INTENSITY_50 error (mm)	Mean INTENSITY_SUM error (mm)	Mean area error (km^2)	Mean CENTROID_DIST (km)	Bias*	ETS
Control	0.0000	-0.04	-2425.09	-1661.15	0.00	0.99546	0.00000
KF orig	0.0294	-0.80	-623.34	-862.09	8.58	0.99569	-0.00797
KF nodx	0.0098	-0.83	6745.61	1701.17	6.89	1.10120	-0.01508
KF 5x5 ave WTQ	-0.0335	-1.85	-1044.48	-816.02	5.25	1.48302	-0.02328
KF 5x5 ave tend	0.0103	-1.16	5681.63	3069.35	11.97	1.17426	-0.00972

Table 2b. As in Table 2a except for standard deviation.

Run	MMI	Mean INTENSITY_50 error (mm)	Mean INTENSITY_SUM error (mm)	Mean area error (km^2)	Mean CENTROID_DIST (km)	bias*	ETS
Control	0.0000	1.87	8885.40	3329.25	0.00	0.35297	0.00000
KF orig	0.0866	2.07	11601.16	4164.98	33.04	0.51369	0.02259
KF nodx	0.0596	4.58	27612.82	7802.84	52.69	1.00167	0.04038
KF 5x5 ave WTQ	0.0485	1.25	19464.36	6259.40	64.38	1.18970	0.04820
KF 5x5 ave tend	0.0817	2.48	26213.99	9927.15	40.18	0.67513	0.03812

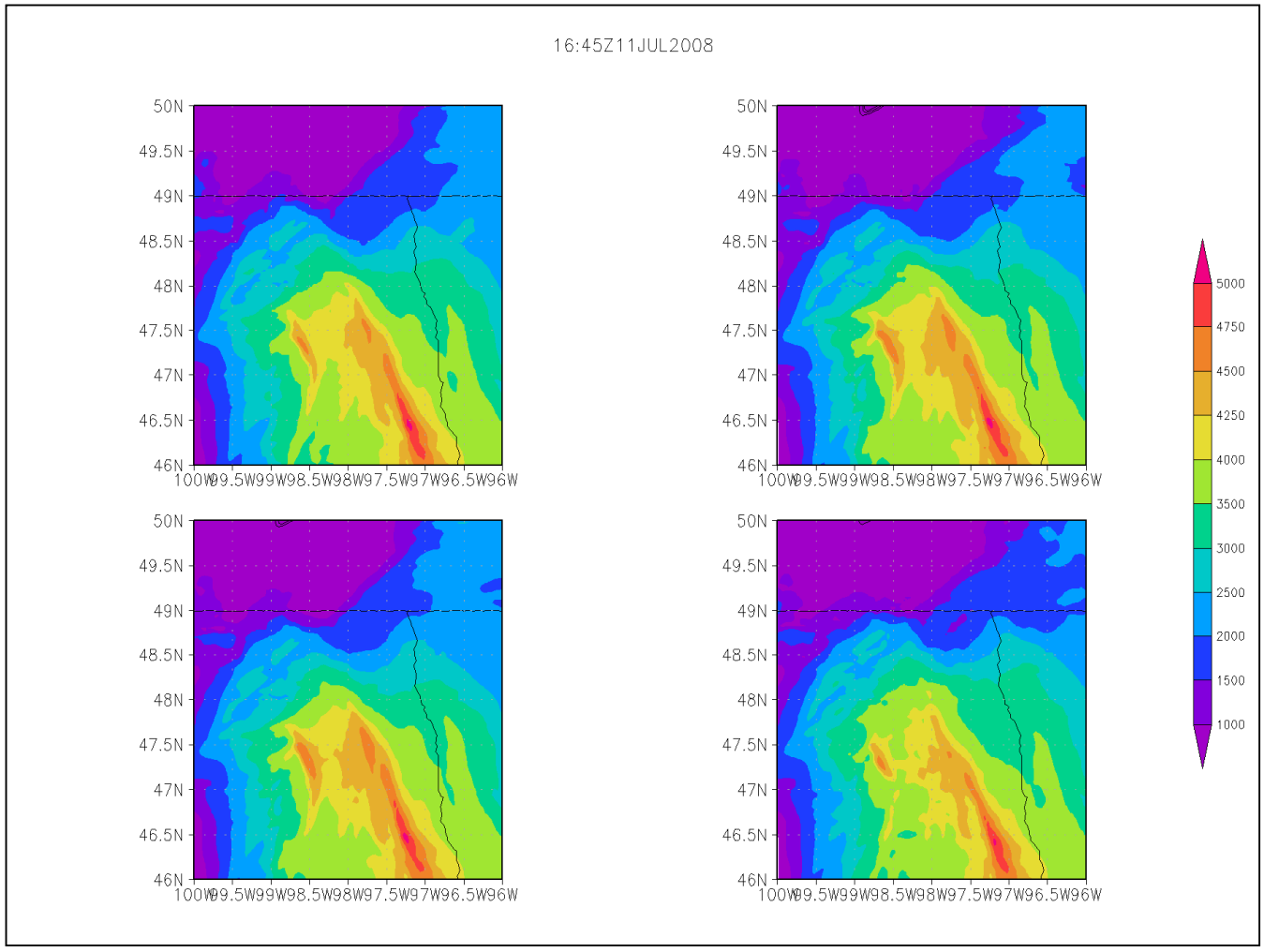

Figure 3. Most unstable CAPE (J/kg) at 1645 UTC 11 July 2008 for a region in northwest Minnesota and the eastern Dakotas just before convective initiation is color filled. The different runs shown from bottom left, clockwise: KF orig, KF nodx, KF 5x5 ave tend, KF 5x5 ave WTQ.

by the changes in the KF trigger function.

Vertical profiles of area-averaged omega (the averaging area was a 4° x 4° latitude/longitude box centered on the centroid of 1-hr precipitation at initiation) show no systematic difference between the different runs. In many cases, there was very little difference in the magnitude of omega in the 900 – 700 mb layer. In other cases, one or two of the runs had stronger or weaker vertical motion in that layer, but no single run type was consistently stronger or weaker than the others.

Detailed analyses of other fields such as most unstable CAPE, CIN, surface divergence, 700 mb omega, surface temperature, and surface dewpoint, also revealed very little in the way of differences between the different run types. In fact, in some cases and for some fields, the differences were nearly imperceptible. The same features (e.g., a surface outflow boundary or other convergent boundary, a tongue of most unstable CAPE, or a moist axis at the surface) were present in each run for a given case. When there was a difference, it usually was a matter of a small difference in magnitude. An example of this is shown in Fig. 3. Initiation is about to occur near the center of the panels in Fig. 3. It occurs at different times in each of the runs (there are nearly two hours between earliest and latest initiation), yet the most-unstable CAPE shows the exact same features with only minute differences in the shape of the instability tongue and the magnitude of most unstable CAPE within the tongue.

Despite the previous discussion noting the difficulties in discovering differences between the different runs which may explain

their behavior regarding convective initiation, a few systematic behaviors were found among the different runs regarding precipitation. Of the 3 mm of 1-hr precipitation required to define convective initiation, it was found that the majority of that precipitation, if not the entirety of it, came from the KF scheme in the KF 5x5 ave WTQ run in every case, and in the KF 5x5 ave tend and KF nodx runs in a large number of cases, but not in every one. This was especially the case when a run initiated convection early. Also, when this happened, it was also common for there to be a several hour delay in production of precipitation by the Thompson scheme in the KF 5x5 ave WTQ run. This tendency was also seen in the KF 5x5 ave tend and KF orig runs, but with a shorter delay. On the other hand, there was much more balance between the Thompson and KF schemes in producing precipitation at initiation in the KF orig run. The handling of the trigger function in the KF scheme likely explains most of this behavior for the KF 5x5 ave WTQ and KF nodx schemes. The trigger function was not altered in the KF 5x5 ave tend run, so an alternate explanation for the behavior of precipitation in that run is required. This explanation likely includes the averaging of convective time-step precipitation, effectively smearing precipitation over a wider area each time the KF scheme activates. This finding is supported by the portion of total precipitation in a 24-hr period that came from the KF scheme. The KF 5x5 ave WTQ run had largest with an average of 70% of 24-hr precipitation coming from the KF scheme, followed by the KF 5x5 ave tend run with an average of 53%. The KF nodx and KF orig averaged 49% and 26%, respectively, indicating that the KF scheme was doing most of the "work" in the runs with modified KF code, while the Thompson scheme was doing most of the work in the unmodified KF run (the KF orig run).

5. Summary and conclusions

This study attempted to determine whether there is added forecast skill when the KF scheme is used in a high-resolution mesoscale model. The WRF-ARW, version 3.1.1, was used to simulate the initiation of 12 warm-season MCSs using a grid spacing of 3 km. Five different types of simulations were conducted for each of the cases: one of them used no CPS (control), while the other four used the KF scheme with code modifications to three of them (KF nodx, KF 5x5 ave WTQ, and KF 5x5 ave tend) to determine if those runs would also improve forecast skill.

Analysis of skill scores derived through the use of MODE for 1-hr and 6-hr accumulated precipitation starting at initiation showed that in general there is no systematic indication that the modified KF runs forecasted initiation better than the KF orig and control run, although the KF 5x5 ave tend run did forecast initiation well, but not 6-hr precipitation. The skill scores also showed that the KF orig run compares well with the control run, suggesting that indeed there may be some added forecast skill with the use of the KF scheme even at such high resolution. However, the sample size in this project was rather small and the spread in the scores was very large, so nothing statistically significant can be concluded about the results of this study. This can be addressed by adding more cases in the future.

The treatment of the trigger function in the KF scheme likely played a role in the difference in behavior between the modified and unmodified KF runs at initiation. However, it remains to be seen just how much affect the treatment of the trigger function had on initiation versus how the rest of the KF scheme treated the code modifications. This can be addressed by conducting a factor separation experiment (Stein and Alpert 1993) using grid spacing in the trigger function and the other code changes as factors.

Although a fairly detailed analysis of soundings, vertical profiles of omega, and various other fields indicated very little differences between the various runs around the time of initiation, it will likely be beneficial to conduct an even finer-scale analysis of these fields, as initiation of convection is very sensitive to low-level thermodynamic and kinematic fields, and it may be the case that a 1 K difference in surface temperature or surface dewpoint, a 50 Jkg^{-1} difference in CAPE, a $1x10^{-5}$ s^{-1} difference in surface divergence, or a 1 μbs^{-1} difference in omega at some level in the lower troposphere may be enough of a difference to cause a difference in initiation location and/or timing on the order of minutes to hours and on the order of 10's of kilometers.

Lastly, the definition of convective initiation used in this study was the first time at which 1-hr accumulated precipitation reached 3 mm. This definition is probably not the best such definition in theory, but it is easy to enforce. Given that deep moist convection first originates as an unstable parcel of air first breaks through a layer of inhibition and

accelerates vertically through the troposphere, perhaps there are better ways to define initiation, such as a threshold on cloud-water or rain-water mixing ratio in a location, or magnitude of vertical motion over a depth of the troposphere. The temporal and spatial resolution of model data will dictate the best definition to use. While the definition used in this study may be appropriate for time and length scales on the order of tens of minutes to hours and several kilometers, other definitions mentioned may require information on time and length scales on the order of minutes or sub-minutes and on the order of a few kilometers or hundreds of meters.

6. Acknowledgements

The authors would like to thank those who helped in the research process, including Eric Aligo and wrfhelp for help with WRF coding, and John Halley Gotway and Tara Jensen for help running MODE. Stage IV data were provided by NCAR/EOL under sponsorship of the National Science Foundation. This work was funded by NSF grant ATM-0848200, with funds from the American Recovery and Investment Act of 2009.

7. References

Bryan, G. H., J. C. Wyngaard, and J. M. Fritsch, 2003: Resolution requirements for the simulation of deep moist convection. *Mon. Wea. Rev.*, **131**, 2394-2416.

Fritsch, J. M., and C. F. Chappell, 1980: Numerical prediction of convectively driven mesoscale pressure systems. Part I: Convective parameterization. *J. Atmos. Sci.*, **37**, 1722-1733.

Gilliland, E. K., and C. M. Rowe, 2007: A comparison of cumulus parameterization schemes in the WRF model. Preprints, *21st Conf. on Hydrology*, San Antonio, TX, Amer. Meteor. Soc., P2.16.

Kain, J., 2004: The Kain-Fritsch convective parameterization: an update. *J. App. Meteor.*, **43**, 170-181.

Lean, H. W., P. A. Clark, M. Dixon, N. M. Roberts, A. Fitch, R. Forbes, and C. Halliwell, 2008: Characteristics of high-resolution versions of the Met Office Unified Model for forecasting convection of the United States. *Mon. Wea. Rev.*, **136**, 3408-3424.

Ma, L.-M., and Z.-M. Tan, 2009: Improving the behavior of the cumulus parameterization for tropical cyclone prediction: convection trigger. *Atmos. Res.*, **92**, 190-211.

Molinari J., and M. Dudek, 1992: Parameterization of convective precipitation in mesoscale numerical models: a critical review. *Mon. Wea. Rev.*, **120**, 326-344.

Stein, U., and P. Alpert, 1993: Factor separation in numerical simulations. *J. Atmos. Sci.*, **50**, 2107-2115.

Wang, W., and N. L. Seaman, 1997: A comparison study of convective parameterization schemes in a mesoscale model. *Mon. Wea. Rev.*, **125**, 252-278.